


RESEARCH

Open Access



DWI and ADC value versus ADC ratio in the characterization of solid renal masses: radiologic-pathologic correlation

Mohamed Samir Shaaban¹, Viviane George Adly Ayad^{1*} , Mohamed Sharafeldein², Mona A. Salem³, M. A. Atta² and Adel A. Ramadan¹

Abstract

Background: Renal masses are becoming an increasingly common finding on cross-sectional images. Characterization of the nature of the lesion either neoplastic or not, benign or malignant as well as further subtype characterization is becoming an important factor in determining management plan. The purpose of our study with to assess the sensitivity and specificity of both ADC mean value and ADC ratio in such characterization along with the calculation of different cutoff values to differentiate between different varieties, using pathological data as the main gold standard for diagnosis.

Results: Our study included 50 patients with a total of 72 masses. A final diagnosis was reached in 69 masses by pathological examination and three masses had clinical and laboratory signs of infection. We had a total of 49 malignant lesions (68%) and 23 benign lesions (32%). The ADC value of ccRCC ($1.4 \times 10^{-3} \text{ mm}^2/\text{s}$) was significantly higher than all other renal masses. A cutoff ADC value of > 1.1 and a cutoff ADC ratio of > 0.56 can be used to differentiate between clear cell renal cell carcinoma and other lesions and an ADC value of < 0.8 and an ADC ratio of ≤ 0.56 to differentiate papillary renal cell carcinoma from other masses. There was no statistically significant ADC value to differentiate between benign and malignant lesions but a statistically significant ADC ratio (> 0.52) was reached.

Conclusion: ADC value and ADC ratio can be used as an adjunct tool in the characterization of different renal masses, with ADC ratio having a higher sensitivity, which can affect the prognosis and management of the patient.

Keywords: Kidney, Neoplasm, Diffusion-weighted imaging, ADC value, ADC ratio

Background

Renal cancer is one of the top ten common types of cancer, 90% of which are renal cell carcinoma (RCC) [1], and thus having a significant impact on health [2].

Many renal cell carcinomas are diagnosed incidentally as they tend to be asymptomatic or may present with symptoms unrelated to the kidneys [1]. The increase in cross-sectional abdominal imaging has led to an increase in the number of incidentally discovered renal masses

[3], most of these masses are small renal masses ($< 4 \text{ cm}$), and out of these 20 percent are benign [4].

With regard to RCC, 75% are clear cell (ccRCC), 7% to 15% are papillary (pRCC), and 5% are chromophobe (chrRCC) subtypes. Collecting duct and medullary carcinomas is rare and account for $< 1\%$ of the renal tumors. The variable histopathologic types are associated with different degrees of aggressiveness and variable prognosis [3, 5]. Clear cell renal cell carcinoma (ccRCC), the most common RCC subtype, has the greatest potential for aggressive behavior among the common subtypes [6].

* Correspondence: vivianegeorge@yahoo.com

¹Department of Diagnostic and Interventional Radiology, Faculty of Medicine, Alexandria University, Alexandria, Egypt
Full list of author information is available at the end of the article

Therefore, it is important to distinguish between the subtypes of renal tumors since each subtype has different tumor behavior as well as different prognosis [7]. Characterization of renal tumors is critical to determine the best therapeutic approach and improve overall patient survival [8].

Furthermore, the distinction between benign from malignant lesions is crucial in deciding on the therapeutic approach; small malignant renal masses are usually surgically removed or treated with minimally invasive percutaneous procedures, whereas benign renal masses are managed conservatively [9].

The most common benign renal tumor is angiomyolipoma which is a mesenchymal tumor consisting of blood vessels, smooth muscle, and adipose tissue. The amount of fat varies between angiomyolipomas, and up to 5% are classified as fat poor, which can mimic malignant renal neoplasms. Another common benign renal tumor is oncocytoma, also known to mimic RCC on imaging [3, 5].

Diffusion-weighted imaging (DWI) sequences characterize the restriction of the random (Brownian) movement of water molecules within tissues [10]. It is a non-invasive technique, capable of probing the structure of biologic tissues at a microscopic level, and thus can be used for in vivo tissue characterization [11].

Many researchers have reported increased diagnostic value when using DWI for tumor differentiation in the differential diagnosis of cerebral tumors [12], whereas other researchers have investigated the use of DWI in differentiating between benign and malignant pediatric abdominal tumors [13] as well as in the characterization of focal liver lesions [14] and many other body organs.

The ratio between the ADC value of the renal mass and the ADC value of the normal renal parenchyma has been proposed as a potential parameter to differentiate between benign and malignant renal masses as well as to help in the characterization of the different subtypes of renal tumors.

We conducted this study to investigate diffusion weighted imaging as non-invasive non-enhanced tool in the differentiation between benign and malignant renal tumors as well as the characterization of the different types of renal masses, using both the ADC value of the different renal masses as well as the ratio between the mass ADC and the renal parenchyma ADC as different parameters to help in characterization of renal masses.

Methods

Subjects

This was a prospective study performed in patients with suspected solid renal masses identified on either computed tomography or ultrasound and presented for further characterization, between January 2018 and June 2020. Patients with suspected lesions on ultrasound

proved by MRI to be cystic (Bosniak 1 and 2) as well as patients with pseudo-lesions were excluded from the study. Cases of lipid-rich AML were easily diagnosed visually by CT and US and were not part of our study. Thus, the study included 50 patients with a total of 72 masses.

Institutional approval was obtained before the study and patient consent to participate in the study was collected.

MRI technique

The study was performed on a 3-tesla MRI machine (Ingenia, Philips—Netherlands), using body coils with digital broadband technology “dStream architecture.”

Our protocol consisted of T1WI in the axial plane (TR 550 ms, TE 16 ms, slice thickness 3 mm, zero interslice gap, matrix 400×235 , FOV 360×330 mm, NAS 1) and T2WI in the axial plane (TR 1100 ms, TE 80 ms, slice thickness 3 mm, zero interslice gap, matrix 280×220 , FOV 330×300 mm, NAS 1) as well as fat-suppressed T2 sequences in the axial and coronal planes (TR 1100 ms, time to echo TE 80 ms, slice thickness 3 mm, zero interslice gap, matrix 280×220 , FOV 350×330 mm, NAS 1). Diffusion-weighted imaging (DWI) with 3 *b* values (0, 400, and 800) and generated acquired diffusion coefficient (ADC) images (TR 1900 ms, TE 82 ms, slice thickness 3 mm, zero interslice gap, matrix 280×220 , FOV 450×400 mm, NAS 1).

The ADC values were calculated by placing ROI on the lesion when solid or the solid parts of the lesion when having a mixed appearance excluding areas of necrosis. Identical ROIs were placed upon the normal renal parenchyma to calculate the ADC of the renal parenchyma, and the ratio between the ADC of the mass to the ADC of the parenchyma was calculated by dividing the ADC value of the mass by the ADC value of the renal parenchyma.

The images were analyzed by two readers, specialized in uro-radiology (with > 15 years of experience in uro-radiology). Differences between the two readers were solved by consensus.

Statistical analysis

Data were fed into the computer and analyzed using the IBM SPSS software package version 20.0. Qualitative data were described using number and percent. Quantitative data were described using range (minimum and maximum), mean, standard deviation, and median. The significance of the obtained results was judged at the 5% level. ROC curves were plotted using the MedCalc software version 15.8, calculating recommended cutoff values with corresponding sensitivity, specificity, positive predictive value, and negative predictive value.

Final diagnosis

Final diagnoses were reached in all cases based on clinical and laboratory data, pathological analysis when feasible, and follow-up of the patients.

Results

Our study included 50 patients with a total of 72 masses; our patients were 32 males and 18 females, aged between 20 and 75 years old.

The most common presenting symptom was loin pain followed by hematuria. Other symptoms included fever, easy fatigue, loss of appetite, or a combination of more than one symptom. Ten cases were incidentally discovered during abdominal imaging for non-related complaints.

Twenty-three of the masses examined were small renal masses (≤ 4 cm) with 31 masses between 4 and 7 cm, 10 masses between 7 and 10 cm, and 8 masses larger than 10 cm.

The behavior of the masses was assessed in terms of local invasion, distant metastasis, nodal metastasis, and invasion of the pelvicalyceal system (PCS); nine masses were associated with local extra-renal invasion, and three with local and distant metastasis. Twenty masses were associated with invasion of the pelvicalyceal system and eight masses associated with regional lymph nodes.

The final diagnosis was reached based on clinical, laboratory, pathological analysis, and follow-up of the patients; three cases with clinical and laboratory signs of infection were subjected to medical treatment and followed up until symptoms resolution, and were diagnosed as infection. Twelve masses were diagnosed after core needle biopsy as follows; two of which were in a patient who had a history of urinary bladder carcinoma treated with local instillation of BCG and pathology revealed renal tuberculous granuloma, two other masses were described as advanced-stage renal cell carcinoma based on imaging and were pathologically diagnosed as ccRCC, the last eight were in two patients with history of tuberous sclerosis, core biopsy was undertaken for renal masses with no visible fat on imaging and were pathologically diagnosed as lipid-poor angiomyolipomas. Finally, the remaining 57 masses were diagnosed by pathological examination after excision of the mass (partial or radical nephrectomy). We had a total of 49 malignant lesions (68%) and 23 benign lesions (32%). The final diagnosis is illustrated as follows in Table 1.

The characteristics of different masses were assessed on DWI/ADC, with 67 out of 72 masses showing restricted diffusion. The mean, median, maximum and minimum ADC value, and ADC ratio were calculated for each diagnostic category (Tables 2 and 3), as well as comparing the mean ADC value and ADC ratio for each mass (Table 4).

Table 1 The final diagnosis for the studied masses ($n = 72$)

	No.	%
Definite diagnosis ($n = 72$)		
Clear cell RCC	27	37.5
Papillary RCC	15	20.8
AML	12	16.7
Oncocytoma	4	5.6
Chromophobe	4	5.6
Infection	3	4.2
T.B nephritis	2	2.8
Metanephric adenoma	2	2.8
Sarcoma	1	1.4
TCC	1	1.4
Collecting duct carcinoma	1	1.4

ROC curves for calculating different cutoff points to reach a cutoff value for differentiating different masses were also calculated.

Various ROC curves were computed using both ADC value and ADC ratio to characterize the different lesions.

ROC curves were computed to reach a cutoff point to differentiate between neoplastic and non-neoplastic lesions; cases of infections (non-neoplastic) showed lower ADC value and ADC ratio than neoplastic lesions, also using ADC ratio had higher sensitivity than the ADC value.

Cutoff ADC value of $> 0.85 \times 10^{-3} \text{ mm}^2/\text{s}$ can be used to differentiate neoplastic from non-neoplastic lesions with a sensitivity of 69.35% and specificity of 60.0%, a negative predictive value of 13.6%, and a positive predictive value of 95.6% ($p = 0.045$) (Fig. 1).

Cutoff ADC ratio of $> 0.41 \times 10^{-3} \text{ mm}^2/\text{s}$ to diagnose neoplastic from non-neoplastic lesions can be used with a sensitivity of 85.48% and specificity of 80.00%, a negative predictive value of 30.8%, and a positive predictive value of 98.1% ($p = 0.003$) (Fig. 2).

A statistically significant cutoff value to differentiate between benign and malignant neoplastic lesions was not reached using the ADC values, yet using the ADC ratio had a statistically significant cutoff point.

Cutoff ADC ratio of $> 0.52 \times 10^{-3} \text{ mm}^2/\text{s}$ can be used to diagnose malignant from benign neoplastic lesions with a sensitivity of 65.31% and specificity of 92.1%, a negative predictive value of 41.1%, and a positive predictive value of 97% ($p = 0.038$) (Fig. 3).

A cutoff value was calculated to differentiate between clear cell RCC from other lesions showing diffusion restriction using ADC value and ACD ratio in order, with the ADC ratio showing more sensitivity.

Cutoff ADC value of $> 1.1 \times 10^{-3} \text{ mm}^2/\text{s}$ to differentiate cases of clear cell RCC from other tumors can be

Table 2 Min., max., mean, and median ADC for different masses ($n = 67$)

Definite diagnosis	N	ADC		
		Min.-max. ($\times 10^{-3} \text{ mm}^2/\text{s}$)	Mean \pm SD. ($\times 10^{-3} \text{ mm}^2/\text{s}$)	Median ($\times 10^{-3} \text{ mm}^2/\text{s}$)
Clear cell RCC	27	0.80-1.60	1.4 ± 0.19	1.20
Papillary RCC	15	0.50-1.10	0.80 ± 0.18	0.80
AML	9	0.70-1.10	0.89 ± 0.16	0.85
Chromophobe RCC	4	0.70-1.0	0.85 ± 0.13	0.85
Oncocytoma	3	0.90-1.40	1.10 ± 0.26	1.0
Infection	3	0.80-0.90	0.87 ± 0.06	0.90
Tuberculoma	2	0.70-0.70	0.70 ± 0.0	0.70
TCC	1		1.10	
Sarcoma	1		0.90	
Metanephric adenoma	1		1.0	
Collecting duct carcinoma	1		0.70	

used with a sensitivity of 72.41% and a specificity of 95.74%, a negative predictive value of 84.9%, and a positive predictive value of 91.3% ($p < 0.001$) (Fig. 4).

A cutoff ADC ratio of $> 0.56 \times 10^{-3} \text{ mm}^2/\text{s}$ to diagnose cases with clear cell RCC from other masses can be used with a sensitivity of 88.89% and specificity of 90%, a negative predictive value of 85.7%, and a positive predictive value of 92.3% ($p < 0.001$) (Fig. 5).

A cutoff value to differentiate between papillary RCC from other lesions showing diffusion restriction was calculated using both ADC value and ACD ratio.

Cutoff ADC value of $\leq 1 \times 10^{-3} \text{ mm}^2/\text{s}$ to diagnose cases with papillary RCC from other cases can be used with a sensitivity of 88.24% and specificity of 49.15%, a negative predictive value of 93.5%, and a positive predictive value of 33.3% ($p < 0.001$) (Fig. 6).

Cutoff ADC ratio of ≤ 0.56 ADC to diagnose cases with papillary RCC from other masses can be used with a sensitivity of 88.67% and specificity of 50%, a negative

predictive value of 92.9%, and a positive predictive value of 33.3% ($p = 0.004$) (Fig. 7).

No statistically significant cutoff value was found to characterize AML from other masses, using neither the ADC value nor the ADC ratio.

Examples of some of the different masses detected by MRI in our study are presented in Figs. 8, 9, 10, and 11.

Discussion

Renal masses are frequently encountered on cross-sectional imaging done either for kidney-related symptoms or as an incidental finding. The increased incidence especially in elderly people and those with multiple co-morbidities warrants the need for a non-invasive tool to characterize those lesions.

Renal cell carcinoma is the most common renal neoplasm and of which clear cell subtype is the most common subtype. Each subtype has a different aggressiveness and thus a different prognosis.

Table 3 Min., max., mean, and median ADC ratio for different masses ($n = 67$)

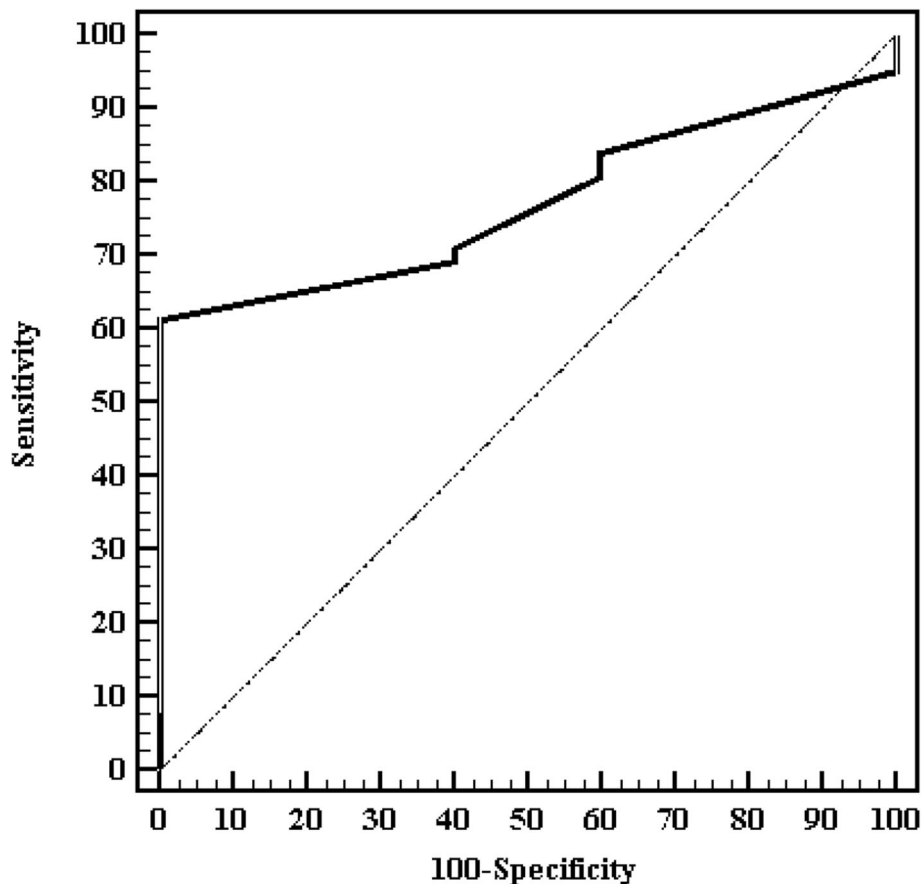
Definite diagnosis	N	ADC ratio		
		Min.-max. ($\times 10^{-3} \text{ mm}^2/\text{s}$)	Mean \pm SD. ($\times 10^{-3} \text{ mm}^2/\text{s}$)	Median ($\times 10^{-3} \text{ mm}^2/\text{s}$)
Clear cell RCC	27	0.44-0.80	0.64 ± 0.07	0.65
Oncocytoma	3	0.47-0.50	0.49 ± 0.02	0.50
Sarcoma	1		0.56	
Abscess	3	0.40-0.42	0.41 ± 0.01	0.41
AML	9	0.37-0.52	0.47 ± 0.05	0.47
Chromophobe	4	0.40-0.46	0.44 ± 0.03	0.45
T.B nephritis	2	0.34-0.35	0.35 ± 0.01	0.35
TCC	1		0.65	
Papillary RCC	15	0.29-0.61	0.45 ± 0.11	0.44
Metanephric adenoma	1		0.62	
Collecting duct carcinoma	1		0.41	

Table 4 Mean ADC value and ADC ratio for different masses ($n = 67$)

Definite diagnosis	N	ADC value Mean \pm SD. ($\times 10^{-3}$ mm ² /s)	ADC ratio Mean \pm SD. ($\times 10^{-3}$ mm ² /s)
Clear cell RCC	27	1.4 \pm 0.19	0.64 \pm 0.07
Oncocytoma	3	0.80 \pm 0.18	0.49 \pm 0.02
Sarcoma	1	0.89 \pm 0.16	0.56
Abscess	3	0.85 \pm 0.13	0.41 \pm 0.01
AML	9	1.10 \pm 0.26	0.47 \pm 0.05
Chromophobe	4	0.87 \pm 0.06	0.44 \pm 0.03
T.B nephritis	2	0.70 \pm 0.0	0.35 \pm 0.01
TCC	1	1.10	0.65
Papillary RCC	15	0.90	0.45 \pm 0.11
Metanephric adenoma	1	1.0	0.62
Collecting duct carcinoma	1	0.70	0.41

Multiple studies aiming at investigating different parameters in a trial to differentiate those subtypes based on imaging were done. Finding a method to distinguish the lesion along with its extensions is important for the management, and as contrast-enhanced studies are not always feasible (either due to patient-related factors or technical difficulties as well as cost-related issues), our study aimed at studying the role of DWI/ADC as a tool in diagnosis and characterization, as well as comparing ADC value and ADC ratio and their roles in the characterization of the renal masses.

ccRCC was the most common subtype with a higher mean ADC than other benign and malignant lesions showing a mean ADC value of $1.4 \pm 0.19 \times 10^{-3}$ mm²/s, and the results are consistent with those by Zhang et al., de Silva et al., Sevcenco et al., Serter et al., and el Serougy et al. reporting mean ADC value of $1.53 \pm 0.31 \times 10^{-3}$ mm²/s [15], 1.50×10^{-3} mm²/s [16], $1.38 \pm 0.56 \times 10^{-3}$ mm²/s [4], $1.474 \pm 0.575 \times 10^{-3}$ mm²/s [17], and $1.56 \pm 0.27 \times 10^{-3}$ mm²/s [18], respectively. Mirka et al. used the median ADC to report their results, reporting a median of 1.365×10^{-3} mm²/s for ccRCC [19], which is

**Fig. 1** ROC curve to assess agreement (sensitivity, specificity) of the ADC value to diagnose neoplastic from non-neoplastic lesions. A cutoff value of $> 0.85 \times 10^{-3}$ mm²/s can be used to differentiate neoplastic from non-neoplastic lesions with a sensitivity of 69.35% and specificity of 60.0%

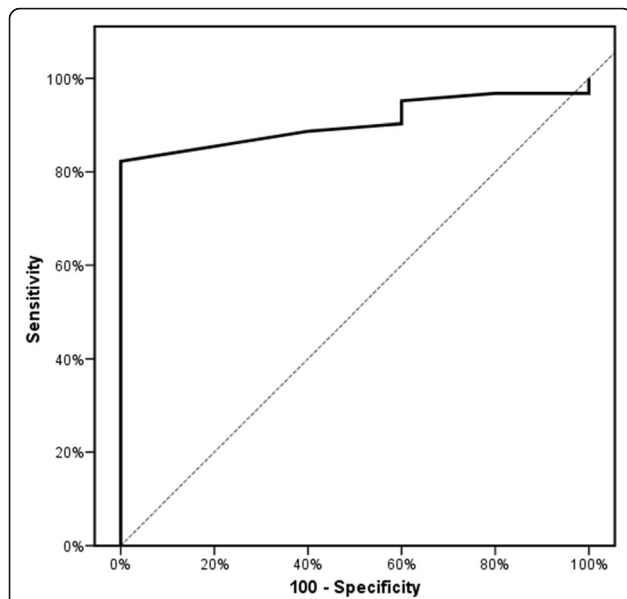


Fig. 2 ROC curve to assess agreement (sensitivity, specificity) of the ADC ratio to diagnose neoplastic from non-neoplastic lesions. Cutoff ADC ratio of $> 0.41 \times 10^{-3} \text{ mm}^2/\text{s}$ to diagnose neoplastic from non-neoplastic lesions can be used with a sensitivity of 85.48% and specificity of 80.00%

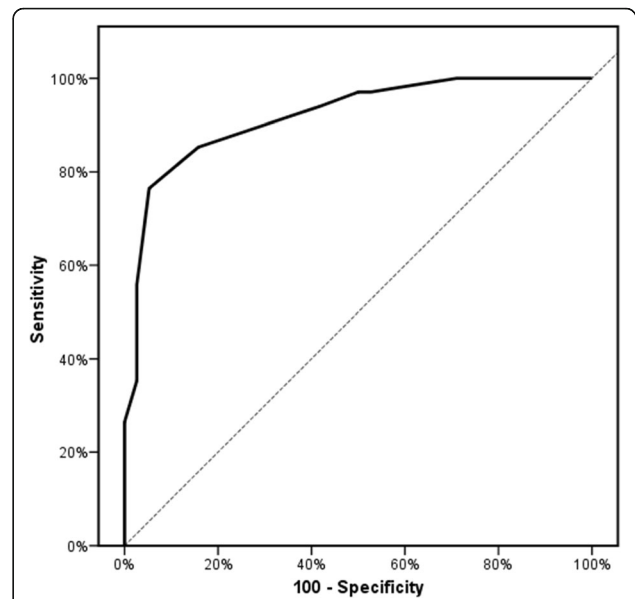


Fig. 4 ROC curve to assess agreement (sensitivity, specificity) of the ADC value to diagnose cases with clear cell RCC from other tumors. Cutoff ADC value of $> 1.1 \times 10^{-3} \text{ mm}^2/\text{s}$ can be used to distinguish cases of clear cell RCC from other tumors with a sensitivity of 72.41% and a specificity of 95.74%

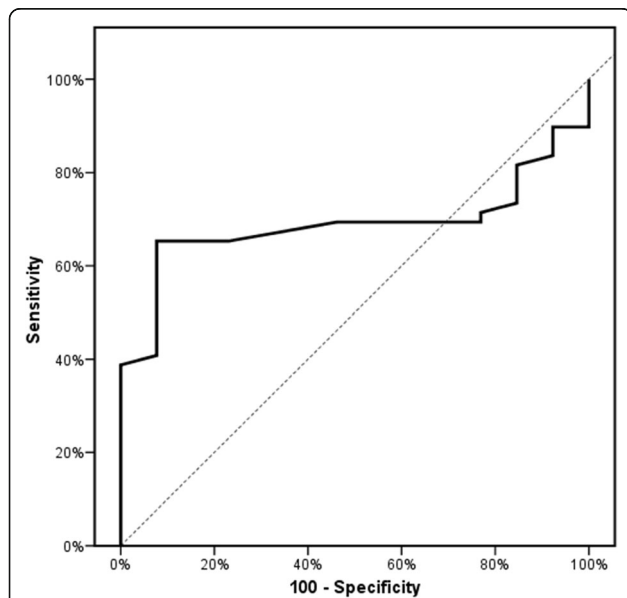


Fig. 3 ROC curve to assess agreement (sensitivity, specificity) of the ADC ratio to diagnose malignant from benign neoplastic lesions. Cutoff ADC ratio of $> 0.52 \times 10^{-3} \text{ mm}^2/\text{s}$ can be used to diagnose malignant from benign neoplastic lesions with a sensitivity of 65.31% and specificity of 92.1%

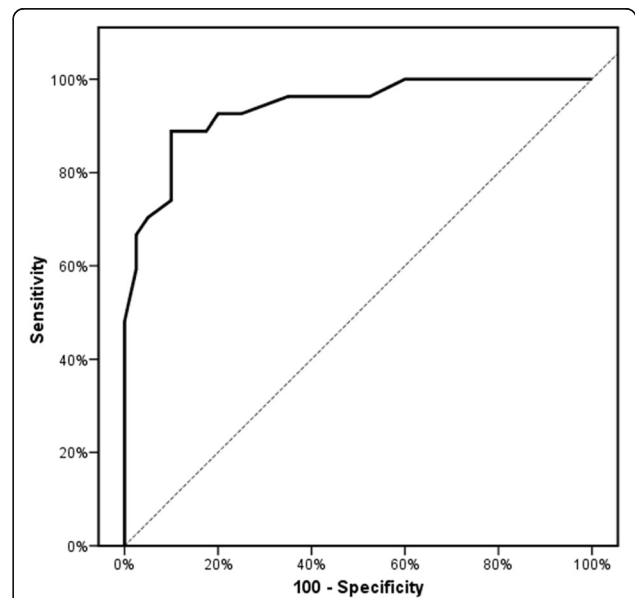


Fig. 5 ROC curve to assess agreement (sensitivity, specificity) of the ADC ratio to diagnose cases with clear cell RCC from other masses. A cutoff ADC ratio of $> 0.56 \times 10^{-3} \text{ mm}^2/\text{s}$ to diagnose cases with clear cell RCC from other masses can be used with a sensitivity of 88.89% and specificity of 90%

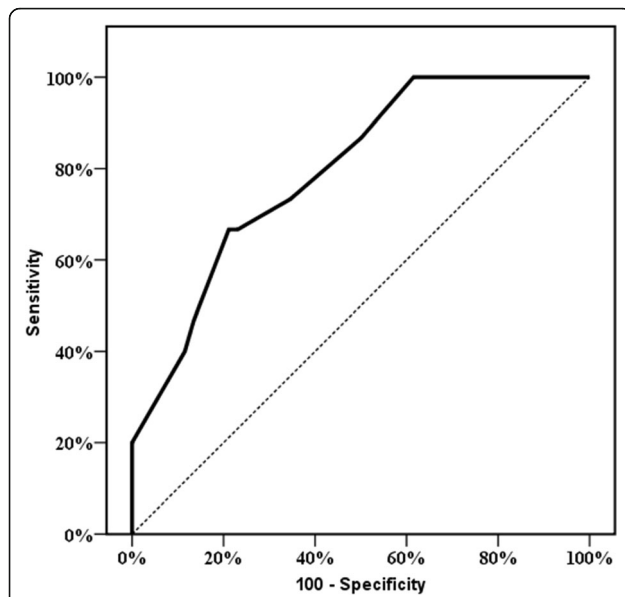


Fig. 6 ROC curve to assess agreement (sensitivity, specificity) of the ADC value to diagnose cases with papillary RCC from other cases (neoplastic and non-neoplastic). Cutoff ADC value of $\leq 1 \times 10^{-3} \text{ mm}^2/\text{s}$ to diagnose cases with papillary RCC from other cases can be used with a sensitivity of 88.24% and specificity of 49.15%

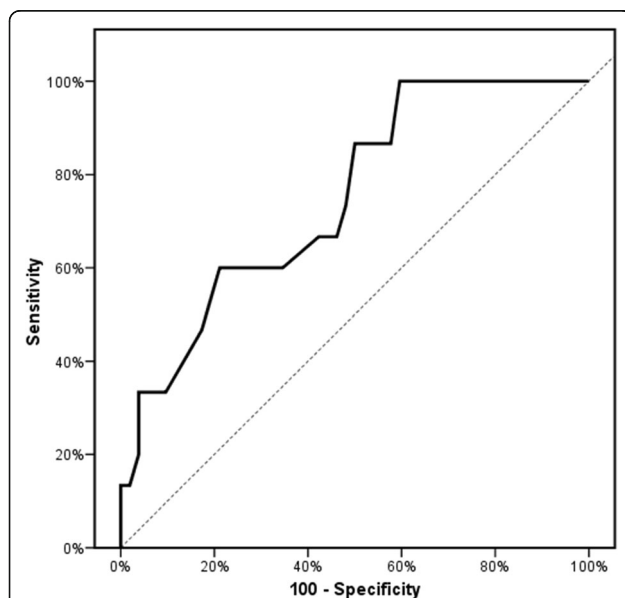


Fig. 7 ROC curve to assess agreement (sensitivity, specificity) of the ADC ratio to diagnose cases with papillary RCC from other masses. Cutoff ADC ratio of ≤ 0.56 ADC to diagnose cases with papillary RCC from other masses can be used with a sensitivity of 88.67% and specificity of 50%

close to our results having a median of $1.2 \times 10^{-3} \text{ mm}^2/\text{s}$ for ccRCC.

Razek et al. had a higher mean ADC for ccRCC of $1.74 \pm 0.12 \times 10^{-3} \text{ mm}^2/\text{s}$ [20], which could be attributed to the fact that their study was conducted on a 1.5T machine whereas ours was performed on a 3T machine, in addition to the different sample sizes (27 cases of ccRCC in our study compared to 19 in the study by Razek et al.).

In our study, we had a mean ADC value for pRCC of $0.80 \pm 0.18 \times 10^{-3} \text{ mm}^2/\text{s}$; results are close to those by de Silva et al., Sevcenco et al., and el-Serougy et al. reporting a mean ADC value of $0.76 \times 10^{-3} \text{ mm}^2/\text{s}$ [16], $1.016 \pm 0.377 \times 10^{-3} \text{ mm}^2/\text{s}$ [4], and $0.96 \pm 0.25 \times 10^{-3} \text{ mm}^2/\text{s}$ [18], respectively. Mirka et al. used the median ADC to report their results, reporting a median of $1.0 \times 10^{-3} \text{ mm}^2/\text{s}$ for pRCC [19], which is close to our results having a median of $0.8 \times 10^{-3} \text{ mm}^2/\text{s}$ for pRCC.

However, Razek et al. had different results reporting a mean ADC value for pRCC of $1.65 \pm 0.26 \times 10^{-3} \text{ mm}^2/\text{s}$ [20], the difference again is likely because their study was conducted on a 1.5T machine while our study was performed on a 3T machine, in addition to the different sample sizes (15 cases of pRCC in our study compared to six in the study by Razek et al.).

In our study, we had nine cases of AML showing restriction with a mean ADC of $0.89 \pm 0.16 \times 10^{-3} \text{ mm}^2/\text{s}$, which aligns with other studies by Emad-Eldin et al. and Sevcenco et al. who reported a mean ADC of $0.95 \pm 0.3 \times 10^{-3} \text{ mm}^2/\text{s}$ [21], and $0.828 \pm 0.227 \times 10^{-3} \text{ mm}^2/\text{s}$ [4], respectively. While Ghoneim et al. and de Silva et al. had different results reporting a mean of $0.75 \times 10^{-3} \text{ mm}^2/\text{s}$ [22] and $0.69 \times 10^{-3} \text{ mm}^2/\text{s}$ [16], respectively, this can be attributed to the difference in magnet strength (both studies performed on 1.5-tesla machine while ours was on 3-tesla machine).

In our study, we had four cases of chrRCC with a mean ADC value of $0.85 \pm 0.13 \times 10^{-3} \text{ mm}^2/\text{s}$, similar to findings by el-Serougy et al. who reported a mean ADC value of $0.89 \pm 0.13 \times 10^{-3} \text{ mm}^2/\text{s}$ [18]. This is incompatible with other studies by de Silva et al., Razek et al., and Sevcenco et al. who reported a mean ADC of $1.11 \times 10^{-3} \text{ mm}^2/\text{s}$ [16], $1.44 \pm 0.12 \times 10^{-3} \text{ mm}^2/\text{s}$ [20], and $1.239 \pm 0.334 \times 10^{-3} \text{ mm}^2/\text{s}$ [4], respectively. This can be attributed to the different magnet strength in the former and the larger sample size in the latter two compared to our study. Mirka et al. used the median ADC to report their results, reporting a median of $1.06 \times 10^{-3} \text{ mm}^2/\text{s}$ for chrRCC [19], this was not in concordance with our calculated median of $0.85 \times 10^{-3} \text{ mm}^2/\text{s}$ for chrRCC; this can be attributed to the small sample size.

In the current study, we had three out of four cases of oncocytoma showing restricted diffusion with a mean ADC value of $1.10 \pm 0.26 \times 10^{-3} \text{ mm}^2/\text{s}$, which is not in

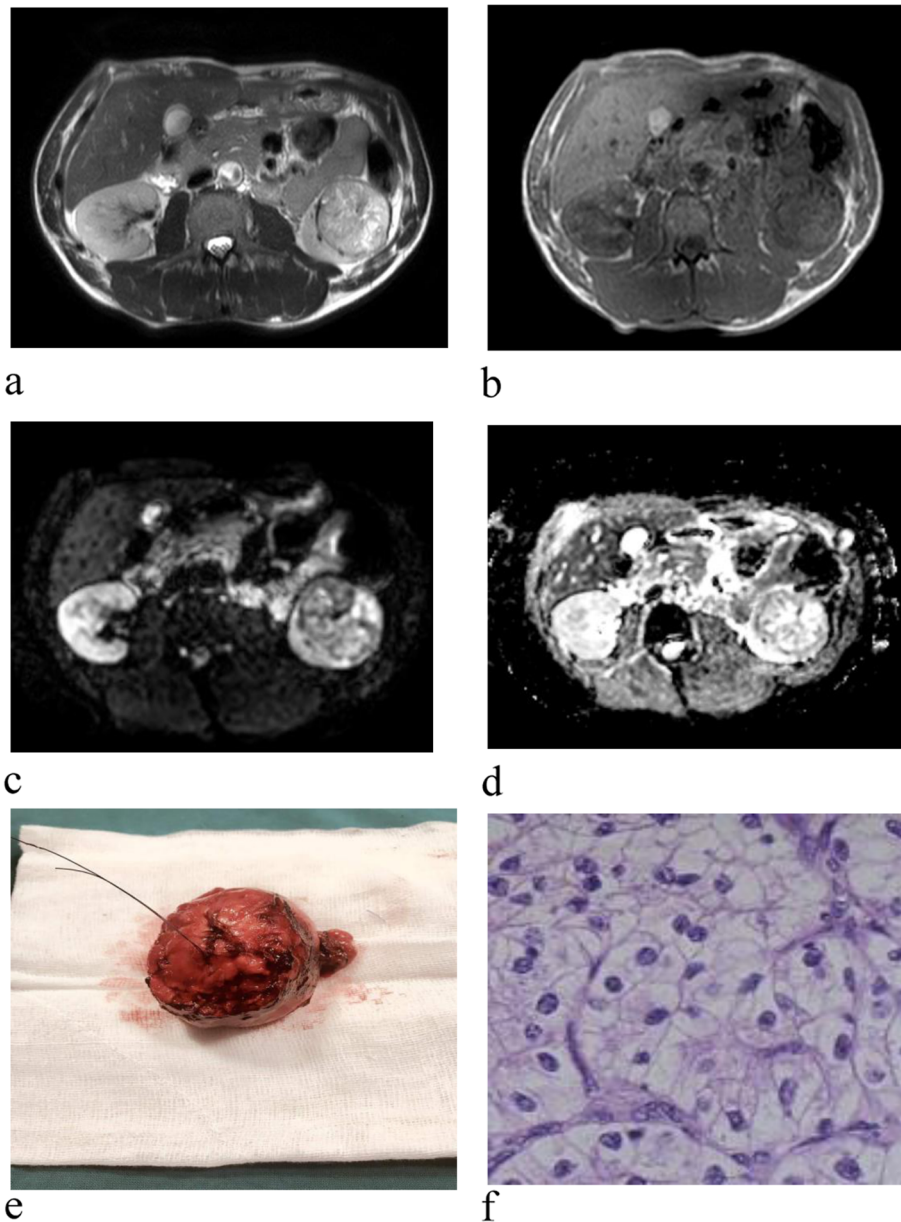


Fig. 8 A 59-year-old male patient with accidental detection of a left renal mass on ultrasound during surveillance for HCC. MRI revealed a left lower zonal heterogeneous mass lesion. **a** T2WI, **b** T1WI, **c** and **d** DWI and ADC showing heterogeneous foci of diffusion restriction, $ADC = 1.4 \times 10^{-3} \text{ mm}^2/\text{s}$, **e** and **f** gross and histo-pathological photograph H&E $\times 400$, clear cell RCC

concordance with other studies by Razeq et al. and Sevcenco et al. who reported a mean ADC of $2.10 \pm 0.10 \times 10^{-3} \text{ mm}^2/\text{s}$ [20], and $1.603 \pm 0.636 \times 10^{-3} \text{ mm}^2/\text{s}$ [4], respectively. This can be attributed to the different magnet power in the former study, and the larger sample size in the latter study. Mirka et al. used the median ADC to report their results, reporting a median of $1.65 \times 10^{-3} \text{ mm}^2/\text{s}$ for oncocytoma [19], this was not in concordance with our study; the median in ours was $1 \times 10^{-3} \text{ mm}^2/\text{s}$, which can be attributed to the different sample size

(three cases in our study and 11 in the study by Mirka et al.).

In our study, we only had one case of TCC which had an ADC value of $1.1 \times 10^{-3} \text{ mm}^2/\text{s}$, and this aligns with the mean calculated in the studies by Ghoneim et al., Emad-Eldin et al., and Sevcenco et al. of $1.1 \times 10^{-3} \text{ mm}^2/\text{s}$ [22], $1.15 \pm 0.3 \times 10^{-3} \text{ mm}^2/\text{s}$ [21], and $1.2 \pm 0.81 \times 10^{-3} \text{ mm}^2/\text{s}$ [4], respectively; each of the studies included 3 cases, as well as the median calculated by Mirka et al. of $1.028 \times 10^{-3} \text{ mm}^2/\text{s}$ [19].

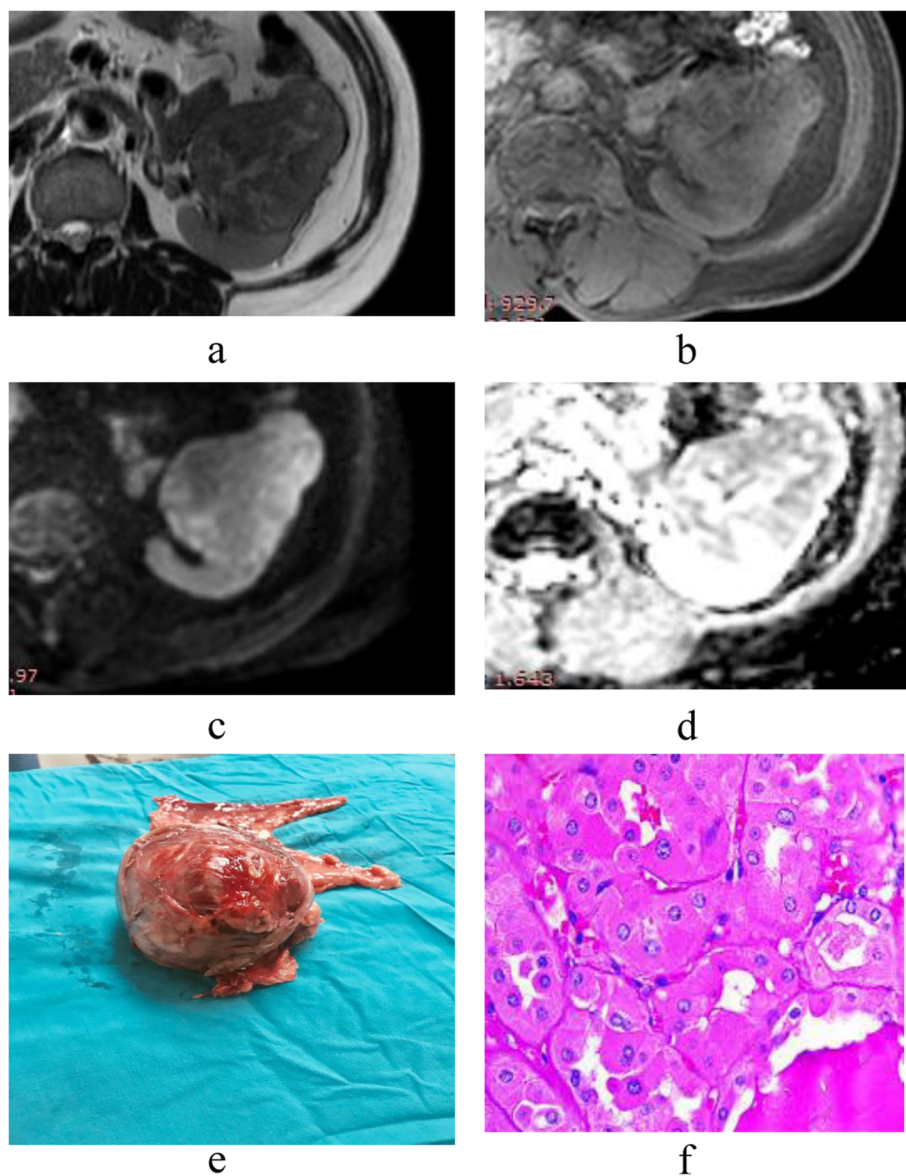


Fig. 9 A 50-year-old female coming with left loin pain **a** T2 WI showing a hypointense left renal mass with central scar, **b** T1WI iso to hypointense, **c, d** DWI with ADC showing restricted diffusion; ADC = $1.18 \times 10^{-3} \text{ mm}^2/\text{s}$, **e** gross surgical specimen after partial nephrectomy, **f** histopathology; oncocytoma; H&E $\times 400$

In our study, we had only three cases of renal infection, with a mean ADC value of $0.87 \pm 0.06 \times 10^{-3} \text{ mm}^2/\text{s}$, and two masses of T.B nephritis with a mean ADC value of $0.70 \times 10^{-3} \text{ mm}^2/\text{s}$.

This is not in concordance with the study by Goyal et al. who reported a mean ADC value for the inflammatory lesions of $1.12 \pm 0.21 \times 10^{-3} \text{ mm}^2/\text{s}$. The difference can be attributed to the different sample sizes (20 cases in their study compared to three cases in our study) [23].

In our study, we only had one case of collecting duct carcinoma; it had an ADC value of $0.7 \times 10^{-3} \text{ mm}^2/\text{s}$.

While Razek et al. had two cases with a higher mean ADC value of $1.1 \pm 0.14 \times 10^{-3} \text{ mm}^2/\text{s}$ [20]. The difference in the ADC value can be attributed to the reason that their study was conducted on a 1.5T machine, whereas our study was performed on a 3T machine.

In our study, we reached a cutoff value to differentiate between neoplastic and non-neoplastic lesions, where a cutoff ADC value of $> 0.85 \times 10^{-3} \text{ mm}^2/\text{s}$ can be used with a sensitivity of 69.35% and specificity of 60.0%, a negative predictive value of 13.6%, and a positive predictive value of 95.6% ($p = 0.045$), and a cutoff ADC ratio of $> 0.41 \times 10^{-3} \text{ mm}^2/\text{s}$ can be used with a sensitivity

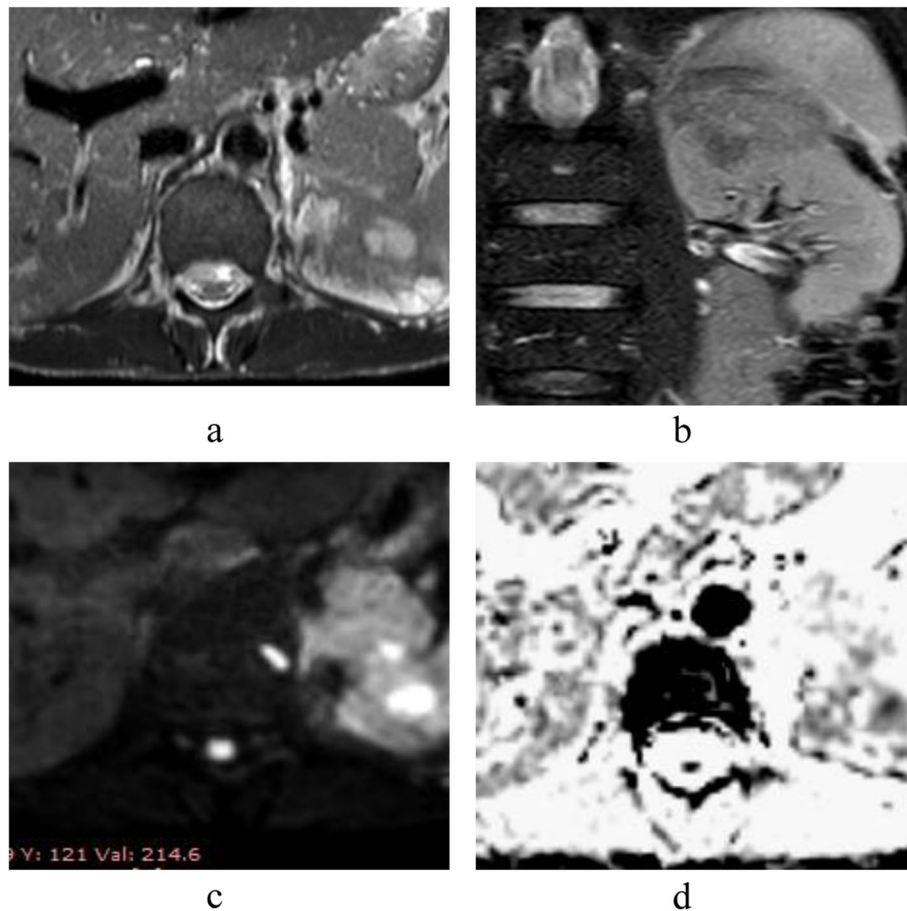


Fig. 10 A 43-years-old male coming with left loin pain, fever, malaise. **a, b** T2 WI axial and sagittal showing a left upper pole heterogeneous lesion with central fluid intensity, **c, d** DWI with ADC showing restricted diffusion among the central fluid; $ADC = 0.8 \times 10^{-3} \text{ mm}^2/\text{s}$

of 85.48% and specificity of 80.00%, a negative predictive value of 30.8%, and a positive predictive value of 98.1% ($p = 0.003$).

None of the previous studies used the ADC ratio in comparing between neoplastic and non-neoplastic lesions.

Also, Goyal et al. showed a statistical difference between inflammatory masses and RCC, however, at a much higher value of $1.41 \times 10^{-3} \text{ mm}^2/\text{s}$, with a sensitivity of 100% and specificity of 78.1%. The difference in the cutoff value could be attributed to the different sample sizes and the fact that our study was conducted on a 3T machine compared to a 1.5T machine in the study by Goyal et al. [23].

Although a cutoff value to differentiate benign and malignant lesions cannot be reached using ADC value, the use ADC ratio calculated a cutoff value of $> 0.52 \times 10^{-3} \text{ mm}^2/\text{s}$ to differentiate between malignant and benign lesions, this can be used with a sensitivity of 65.31% and specificity of 92.1%, a negative predictive value of 41.1%, and a positive predictive value of 97% ($p = 0.038$); this was not in concordance with the study by Ludwig

et al. who reported an ADC ratio of $< 0.89 \times 10^{-3} \text{ mm}^2/\text{s}$ to discriminate malignant from benign lesions, with a sensitivity of 74% and specificity of 78% [24]. This can be attributed to the fact that their study was restricted to T1 hyperintense small lesions while our study had more cases diversity.

Sevcenco et al. in their study also reported no cutoff value between benign and malignant masses using ADC value [4], while Razek et al. reported an ADC value of $1.84 \times 10^{-3} \text{ mm}^2/\text{s}$ as a threshold for differentiating malignant from benign renal tumors, with a sensitivity of 89%, a specificity of 89%, a positive predictive value of 89%, and a negative predictive value of 89% [20], and Ghoneim et al. reported an ADC value of $1.11 \times 10^{-3} \text{ mm}^2/\text{s}$, with a sensitivity of 60%, a specificity of 75%, a positive predictive value of 70.5%, and a negative predictive value of 65.2% [22]. This can be attributed to the difference in magnet strength (1.5 T in both studies compared to 3 T in ours.).

Our findings also contributed to suggesting a cutoff value to help differentiate ccRCC from other neoplastic

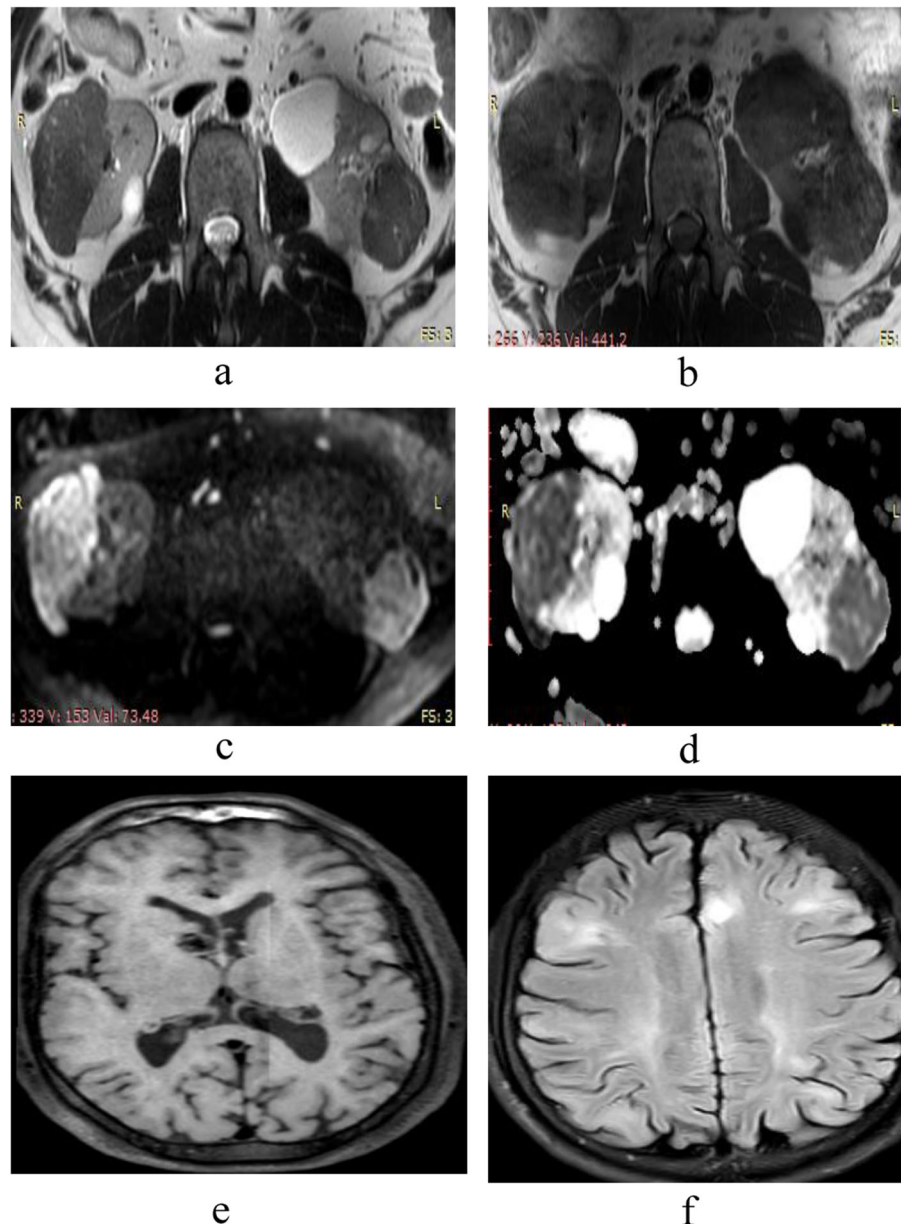


Fig. 11 A 32-year-old male known to have tuberous sclerosis complex **a-d** MRI showing bilateral renal lipid poor AML; **a** T2WI showing bilateral hypointense renal masses, **b** T1WI hypointense, **c, d** DWI with ADC showing restricted diffusion; ADC averaging $0.8-1 \times 10^{-3} \text{ mm}^2/\text{s}$, **e, f** MRI brain of the same patient showing subependymal tubers and white matter changes

lesions; a cutoff value of $> 1.1 \times 10^{-3} \text{ mm}^2/\text{s}$ had a sensitivity of 72.41% and a specificity of 95.74%.

The cutoff value using ADC ratio to differentiate between ccRCC and other masses was $> 0.56 \times 10^{-3} \text{ mm}^2/\text{s}$, with a sensitivity of 88.89% and a specificity of 90%; thus, the ADC ratio is more sensitive with slightly less specificity.

El Serougy et al. calculated a cutoff ADC value in the differentiation between clear cell RCC and non-clear cell RCC of $1.35 \times 10^{-3} \text{ mm}^2/\text{s}$ with a sensitivity of 91.7% and specificity of 76.7%. However, the ADC ratio

demonstrates a cutoff value of $0.64 \times 10^{-3} \text{ mm}^2/\text{s}$ with a sensitivity of 91.7% and a specificity of 81.4% [18]. The difference can be attributed to the diversity of cases in our study including both benign and malignant neoplastic as well as non-neoplastic lesions compared to only RCC subtypes in their study.

De Silva et al. also calculated a cutoff value of differentiate between the different subtypes of RCC, where lesions having ADC value $< 1.3705 \times 10^{-3} \text{ mm}^2/\text{s}$ being more likely a non-clear cell RCC of low malignant potential (chrRCC or pRCC) rather than ccRCC [16].

Again, the difference can be attributed to the diversity of cases in our study including both neoplastic and non-neoplastic lesions.

Razek et al. suggested a cutoff value to differentiate RCC from other renal malignancies, not to differentiate between different subtypes, they used an ADC value of $1.15 \times 10^{-3} \text{ mm}^2/\text{s}$ which revealed an accuracy of 72%, a sensitivity of 95%, a specificity of 50%, a positive predictive value of 66%, and a negative predictive value of 57% [20].

A cutoff value to differentiate pRCC from other neoplastic lesions was also reached in our study by ROC analysis with a value of $\leq 1 \times 10^{-3} \text{ mm}^2/\text{s}$ with a sensitivity of 88.24% and specificity of 49.15%.

This was close to the cutoff value suggested by Sevcenco et al. ($\leq 0.954 \times 10^{-3} \text{ mm}^2/\text{s}$), with a sensitivity of 64.3% and a specificity of 77.1% for the diagnosis of papillary RCC [4].

Using ADC ratio, a cutoff value of $\leq 0.56 \times 10^{-3} \text{ mm}^2/\text{s}$ can be used to differentiate pRCC from other neoplastic lesions with a sensitivity of 88.67% and specificity of 50%, a negative predictive value of 92.9%, and a positive predictive value of 33.3%. This point was not addressed by other studies.

Although in the current study, a pathological correlation was performed for all neoplastic lesions as well as granulomatous lesions, the small sample size along with the paucity of some varieties, such as granulomatous lesions, TCC, and sarcoma, was a limiting factor.

Conclusions

DWI with ADC value is a simple non-invasive and non-enhanced tool that can be used as an adjunct in the characterization of different renal masses, which can greatly affect the prognosis and management of the patient. The use of the ADC ratio add further benefit in differentiating neoplastic from non-neoplastic lesions as well as benign from malignant lesions, it also shows more sensitivity in further RCC subtype characterization.

Abbreviations

RCC: Renal cell carcinoma; ADC: Apparent diffusion coefficient; DWI: Diffusion-weighted imaging; ccRCC: Clear cell renal cell carcinoma; pRCC: Papillary renal cell carcinoma; chrRCC: Chromophobe renal cell carcinoma; AML: Angiomyolipoma; TCC: Transitional cell carcinoma

Acknowledgements

Not applicable.

Authors' contributions

M.S put study design, revised MRI findings, and revised the manuscript writing. V.A collected the patients' data, prepared preliminary reports regarding the findings of MRI in each patient, and wrote the manuscript. A.A revised MRI findings for each patient and revised the manuscript writing. M.A and M.S operated on the patients providing clinical and surgical data as well as gross specimen images. M.S examined the masses for pathology

providing pathological data and histopathological images. All authors read and approved the final manuscript.

Funding

None.

Availability of data and materials

The datasets generated and/or analyzed during the current study are not publicly available due to patient confidentiality but are available from the corresponding author on reasonable request.

Declarations

Ethics approval and consent to participate

Approval was obtained from the IRB at Alexandria University (medical ethics committee) (IRB no. 0007555, FWA no. 00015712). Informed written consent was obtained from all individual participants included in the study.

Consent for publication

All patients included in this research gave written informed consent to publish the data contained within this study (title page).

Competing interests

The authors declare that they have no competing interests.

Author details

¹Department of Diagnostic and Interventional Radiology, Faculty of Medicine, Alexandria University, Alexandria, Egypt. ²Department of Urology, Faculty of Medicine, Alexandria University, Alexandria, Egypt. ³Department of Pathology, Faculty of Medicine, Alexandria University, Alexandria, Egypt.

Received: 23 March 2021 Accepted: 16 July 2021

Published online: 13 August 2021

References

1. Hoang UN, Mirmomen SM, Meirelles O, Yao J, Merino M, Metwalli A et al (2018) Assessment of multiphasic contrast-enhanced MR textures in differentiating small renal mass subtypes. *Abdom Radiol* 43(12):3400–3409. <https://doi.org/10.1007/s00261-018-1625-x>
2. Wu Y, Kwon YS, Labib M, Foran DJ (2015) Singer EA (2015) Magnetic resonance imaging as a biomarker for renal cell carcinoma. *Dis Markers* 2015:648495
3. van Oostenbrugge TJ, Fütterer JJ, Mulders PF (2018) Diagnostic imaging for solid renal tumors: a pictorial review. *Kidney Cancer* 2(2):79–93. <https://doi.org/10.3233/KCA-180028>
4. Sevcenco S, Heinz-Peer G, Ponhold L, Javor D, Kuehhas F, Klingler H et al (2014) Utility and limitations of 3-tesla diffusion-weighted magnetic resonance imaging for differentiation of renal tumors. *Eur J Radiol* 83(6): 909–913. <https://doi.org/10.1016/j.ejrad.2014.02.026>
5. Moch H, Cubilla AL, Humphrey PA, Reuter VE, Ulbright TM (2016) The 2016 WHO classification of tumours of the urinary system and male genital organs—part A: renal, penile, and testicular tumours. *Eur Urol* 70(1):93–105. <https://doi.org/10.1016/j.eururo.2016.02.029>
6. Johnson BA, Kim S, Steinberg RL, de Leon AD, Pedrosa I, Cadeddu JA (2019) Diagnostic performance of prospectively assigned clear cell Likelihood scores (ccLS) in small renal masses at multiparametric magnetic resonance imaging. *Urol Oncol* 37(12):941–946. <https://doi.org/10.1016/j.urolonc.2019.07.023>
7. Wang H-y, Su Z-h XX, Huang N, Z-p S, Wang Y-w et al (2017) Dynamic contrast-enhanced MRI in renal tumors: common subtype differentiation using pharmacokinetics. *Scientif Rep* 7(1):1–10
8. Lopes Vendrami C, Parada Villavicencio C, DeJulio TJ, Chatterjee A, Casalino DD, Horowitz JM et al (2017) Differentiation of solid renal tumors with multiparametric MR imaging. *RadioGraphics* 37(7):2026–2042. <https://doi.org/10.1148/rg.2017170039>
9. Agnello F, Roy C, Bazille G, Galia M, Midiri M, Charles T, Lang H (2013) Small solid renal masses: characterization by diffusion-weighted MRI at 3 T. *Clin Radiol* 68(6):e301–e308. <https://doi.org/10.1016/j.crad.2013.01.002>
10. Lassel E, Rao R, Schwenke C, Schoenberg S, Michael H (2014) Diffusion-weighted imaging of focal renal lesions: a meta-analysis. *Eur Radiol* 24(1): 241–249. <https://doi.org/10.1007/s00330-013-3004-x>

11. Herneth AM, Guccione S, Bednarski M (2003) Apparent diffusion coefficient: a quantitative parameter for in vivo tumor characterization. *Eur J Radiol* 45(3):208–213. [https://doi.org/10.1016/S0720-048X\(02\)00310-8](https://doi.org/10.1016/S0720-048X(02)00310-8)
12. Svolos P, Kousi E, Kapsalaki E, Theodorou K, Fezoulidis I, Kappas C, Tsougos I (2014) The role of diffusion and perfusion weighted imaging in the differential diagnosis of cerebral tumors: a review and future perspectives. *Cancer Imaging* 14(1):20. <https://doi.org/10.1186/1470-7330-14-20>
13. Gawande RS, Gonzalez G, Messing S, Khurana A, Daldrup-Link HE (2013) Role of diffusion-weighted imaging in differentiating benign and malignant pediatric abdominal tumors. *Pediatr Radiol* 43(7):836–845. <https://doi.org/10.1007/s00247-013-2626-0>
14. Okasha A, Wagdy W, Wahman M, Rabea H (2018) Role of diffusion weighted magnetic resonance imaging in diagnosis of hepatic focal lesions. *World J Gastroenterol* 14(46):5805–5812
15. Zhang H-M, Wu Y-H, Gan Q, Lyu X, Zhu X-L, Kuang M et al (2015) Diagnostic utility of diffusion-weighted magnetic resonance imaging in differentiating small solid renal tumors (≤ 4 cm) at 3.0 T magnetic resonance imaging. *Chin Med J* 128(11):1444
16. de Silva S, Lockhart KR, Aslan P, Nash P, Hutton A, Malouf D et al (2021) The diagnostic utility of diffusion weighted MRI imaging and ADC ratio to distinguish benign from malignant renal masses: sorting the kittens from the tigers. *BMC Urol* 21(1):1–7
17. Serter A, Onur MR, Coban G, Yildiz P, Armagan A, Kocakoc E (2020) The role of diffusion-weighted MRI and contrast-enhanced MRI for differentiation between solid renal masses and renal cell carcinoma subtypes. *Abdom Radiol (NY)* 46(3):1041–1052. <https://doi.org/10.1007/s00261-020-02742-w>
18. Elsorougy A, Farg H, Bayoumi D, Abou El-Ghar M, Shady M (2021) Quantitative 3-tesla multiparametric MRI in differentiation between renal cell carcinoma subtypes. *Egypt J Radiol Nuclear Med* 52(1):1–11
19. Mirka H, Korcakova E, Kastner J, Hora M, Hes O, Hosek P, Ferda J (2015) Diffusion-weighted imaging using 3.0 T MRI as a possible biomarker of renal tumors. *Anticancer Res* 35(4):2351–2357
20. Razeq AAKA, Farouk A, Mousa A, Nabil N (2011) Role of diffusion-weighted magnetic resonance imaging in characterization of renal tumors. *J Comput Assist Tomogr* 35(3):332–336. <https://doi.org/10.1097/RCT.0b013e318219fe76>
21. Emad-Eldin S, Rakha S, Hanna SA, Badawy H (2016) Usefulness of diffusion-weighted magnetic resonance imaging for the characterization of benign and malignant renal lesions. *Egypt J Radiol Nuclear Med* 47(1):325–333. <https://doi.org/10.1016/j.ejnm.2015.10.005>
22. Ghoneim SA, Abo Rashid AAE, Nafady HM, Aziz Eldin MMM (2019) Role of diffusion weighted MRI in assessment of renal lesions. *Egypt J Hospital Med* 77(4):5470–5481. <https://doi.org/10.21608/ejhm.2019.59179>
23. Goyal A, Sharma R, Bhalla AS, Gamanagatti S, Seth A (2013) Diffusion-weighted MRI in inflammatory renal lesions: all that glitters is not RCC. *Eur Radiol* 23(1):272–279. <https://doi.org/10.1007/s00330-012-2577-0>
24. Ludwig DR, Ballard DH, Shetty AS, Siegel CL, Yano M (2020) Apparent diffusion coefficient distinguishes malignancy in T1-hyperintense small renal masses. *American J of Roentgenol* 214(1):114–121. <https://doi.org/10.2214/AJR.19.21907>

Publisher's Note

Springer Nature remains neutral with regard to jurisdictional claims in published maps and institutional affiliations.

Submit your manuscript to a SpringerOpen[®] journal and benefit from:

- Convenient online submission
- Rigorous peer review
- Open access: articles freely available online
- High visibility within the field
- Retaining the copyright to your article

Submit your next manuscript at ► [springeropen.com](https://www.springeropen.com)